SUGISAKA MASANORI

Journal of Robotics, Networking and Artificial Life Vol. 9(1); June (2022), pp. 87–92
ISSN (Online): 2352-6386; ISSN (Print): 2405-9021
https://alife-robotics.org/jrnal.html

Research Article

# Efficiency Problem of Spherical Robot in Transfer Kinetic Energy

Kenji Kimura[1], Kazuo Ishii[2]
[1]*Department of Control Engineering, Matsue College of Technology, 14-4, Nishi-ikumacho, Matsue,Shimane, 690-8518, Japan*
[2]*Graduate School of Life Science and engineering, Kyusyu Institute of Technology, 2-4 Hibikino, Wakamatsu-ku, Kitakyushu 808-0196, Fukuoka, Japan*

## ARTICLE INFO

***Article History***

Received 10 November 2020
Accepted 20 June 2022

***Keywords***

Angular velocity vector of the sphere
Angle of sphere rotational axis
Total kinetic energy

## ABSTRACT

Previous spherical mobile robots were driven by two rollers with a fixed rotational axis, which restricts the angular velocity vector of the sphere to two dimensions. Three-dimensional freedom is expected to improve the rotational diversity of the sphere. This study proposes a spherical mobile robot with a variable roller-rotational axis that allows the movement of three degrees of freedom. Furthermore, the kinetic energy of transporting the sphere by the rollers is minimized by an optimization procedure and it is shown that the kinetic energy of sphere transport is efficient.



## 1. Introduction

Many types of robots, such as omnidirectional mobile robots and sphere-transported robots, are based on spherical motions. Therefore, various roller arrangements have been proposed for mobile robot applications.

**Table 1** shows the usage statuses of single spherical robots operated by different mechanisms, and the dimensions of the existence spaces of their angular velocity vectors. **Figure 1** shows the numbers of rollers $N_w$ arranged per wheel in each mechanism, and their contact types.

In the ACROBAT-S [1] mechanism with $N_w = 2$, the caster of each sphere is driven by two roller drives (see **Figure 1** (a)). The wheel chair mechanism [2] has three spheres (**Figure 1** (b)). The rollers are arranged on the equator, generate an angular velocity vector on the horizontal plane, and can move in all directions. The angular velocity vector of the sphere has two-dimensional freedom. This situation is theoretically considered in [3]. In the ball dribbling mechanism [4], the rollers are arranged in the upper hemisphere, where they hold the balls by friction (See **Figure 1** (c)). The two-dimensionality of the sphere's angular velocity vector in these mechanisms was affirmed in kinematic studies of a sphere with slipping [5]. In addition, the kinematics of the reverse motion was verified in a demonstration experiment [6].

Among the three-roller cases ($N_w = 3$), OWMPs [7] deployed in highway maintenance move the spheres within three constrained rollers (See **Figure 1** (d)).The rollers are arranged on the equator parallel to the horizontal plane, and the sphere can be rotated in all directions by generating an angular velocity vector on the plane (note that the existence space of the angular velocity vector is two-dimensional).

A ball-balanced robot [8] has three unconstrained rollers (omni-rollers) arranged in a regular triangular configuration (See **Figure 1** (e)). CPU-Ball Bot [9] has four unconstrained rollers fixed in a square configuration (See **Figure 1** (f)).

*Corresponding Author E-mail: k-kimura@matsue-ct.jp, ishii@brain.kyutech.ac.jp*

In the OWMP, A ball-balanced and CPU-Ball Bot mechanisms [7]-[9], the wheel stands are spherical. In particular, A ball-balanced [8] and CPU-Ball Bot [9] mechanisms can rotate the sphere in three-dimensions using the passive rotation characteristics of the non-rotating direction of the omni-roller.

Such three-dimensional freedom of the angular velocity vector of a sphere will improve the motion diversity of the sphere.

However, unconstrained rollers can slip, degrading the accuracy of the control. Therefore, the use of constraining rollers is desired.

As shown in **Figure 1** (c), this problem can be solved by freeing the rotation axis of the constraining roller, enabling three-dimensional rotation of the sphere.

**Table 1** Existence space of angular velocity vector for sphere mobile robot

| Mechanism | statuses | Rotational Dimension |
|---|---|---|
| ACROBAT-S[1] | Caster | 2 |
| Wheel chair [2] | Wheel | 2 |
| Ball dribbling mechanism [4] | Sphere conveyance | 2 |
| OWMPs [7] | Wheel | 2 |
| A ball-balanced robot [8] | Wheel | 3 |
| CPU-Ball Bot [9] | Wheel | 3 |

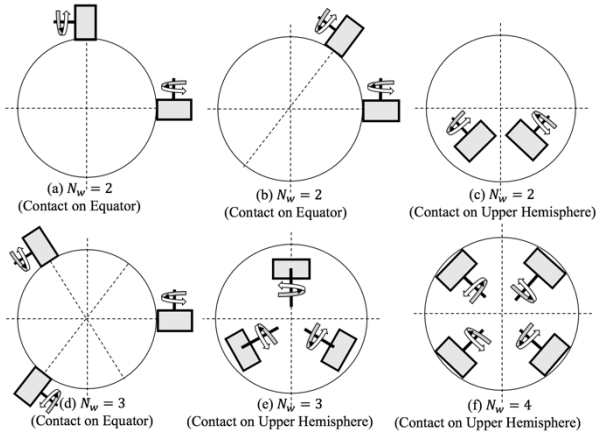


**Figure 1** Type of roller arrangement for sphere mobile robot

the angular velocity vector of a sphere will improve the motion diversity of the sphere. However, a mechanism adapting two constrained rollers is suitable in a spherical object conveyance. It is desired to transport with high kinetic energy efficiency.

In this study, we optimize the total kinetic energy of two rollers. Section 2 calculates the angle of the rotational axis of the sphere, and theoretical formula of minimizes the sum of the kinetic energies of the two rollers. Section 3 presents a simulation of total kinetic energy, and Section 4 summarizes the results and suggests ideas for future work.

## 2. Total kinetic energy

### 2.1 Angular velocity vector of the sphere

The center $\boldsymbol{O}$ of a sphere with radius $r$ is fixed as the origin of the coordinate system $\Sigma - xyz$. The $i^{\text{th}}$ constraint roller ($i$ = 1 or 2) is in point contact with the sphere at a position vector $\boldsymbol{P_i}$ and is arranged such that the center of mass of the roller $\boldsymbol{P_i}$ and $\boldsymbol{O}$ are on the same line. $\boldsymbol{\omega}$ denotes the angular velocity vector of the sphere. $\boldsymbol{\eta_i}$ denotes the unit vector along the rotational axis of constraint roller. sphere direction $\varphi$ ($0° \leq \varphi < 360°$) is the angle from $x$-axis.

Now, given the sphere mobile velocity $\boldsymbol{V}$ (the center velocity of sphere)

$$\boldsymbol{V} = \|\boldsymbol{V}\|[\cos\varphi \quad \sin\varphi \quad 0]^T \tag{1}$$

$\acute{\boldsymbol{\omega}}$ denote orthogonal projection of $\boldsymbol{\omega}$ with respect to $xy$ −plane. $\acute{\boldsymbol{\omega}}$ is perpendicular to $\boldsymbol{V}$ and represented as Equation (2) ($\boldsymbol{V}$ is depend on $\acute{\boldsymbol{\omega}}$).

$$\acute{\boldsymbol{\omega}} = \frac{\|\boldsymbol{V}\|}{r}[-\sin\varphi \quad \cos\varphi \quad 0]^T \tag{2}$$

And. $\acute{\boldsymbol{\omega}}$ is orthogonal projection of $\boldsymbol{\omega}$ with respect to $xy-$ plane.The angle of sphere rotational axis $\rho$ ($-90° \leq \rho \leq 90°$) is the angle between $\boldsymbol{\omega}$ and $\acute{\boldsymbol{\omega}}$. Therefore, $\boldsymbol{\omega} = [\omega_x, \omega_y, \omega_z]^T$ has one-dimensional of freedom with parameter $\rho$ ($\omega_z = \|\boldsymbol{V}\| \tan\rho / r$).

$$\boldsymbol{\omega} = \frac{\|\boldsymbol{V}\|}{r}[-\sin\varphi \quad \cos\varphi \quad \tan\rho]^T \tag{3}$$

Generally, these depend on the orthogonal projection vector of $\boldsymbol{V}$, it has one-dimensional of freedom with respect to $\omega_z = \|\boldsymbol{V}\| \tan\rho / r$.

### 2.2 Kinetic energy of the two rollers

Consider two rollers with radius $R$, moment $I$, and roller's angular velocity $\omega_i$ at $\boldsymbol{P_i}$. The summed kinetic energy of the rollers is given by Eqs.(4).

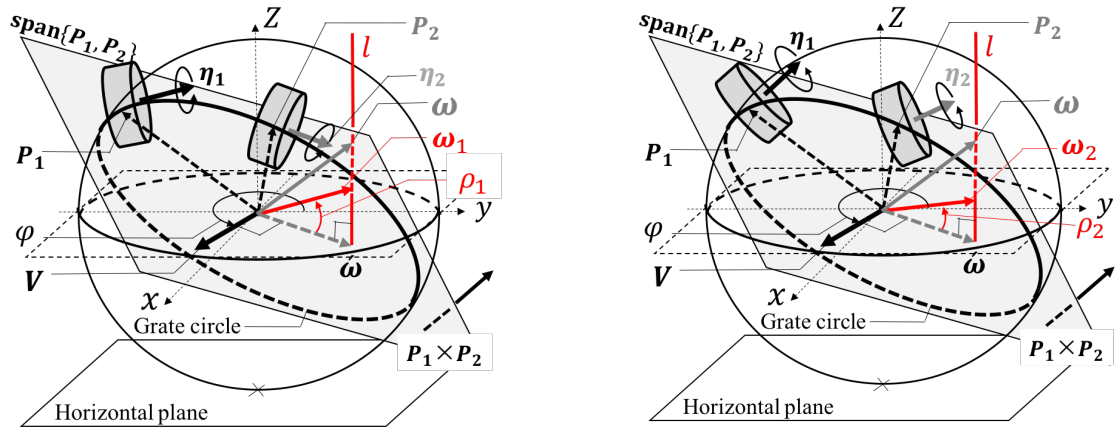


(a) (b)

**Figure. 2** Existence of the sphere angular velocity vector with respect to sphere movile velocity.(a) $\boldsymbol{\omega_1}$ is determined ($\boldsymbol{\omega_1}$ is lay on intersection $\mathbf{span}\{\boldsymbol{P_1}, \boldsymbol{P_2}\}$ and line $\boldsymbol{l}$ . (b) $\boldsymbol{\omega_2}$ is determined as minimizes the summed kinetic energies of the two rollers.

$$E = I(\omega_1^2 + \omega_2^2)$$
$$= \frac{I}{R^2}(\|\boldsymbol{\omega} \times \boldsymbol{P_1}\|^2 + \|\boldsymbol{\omega} \times \boldsymbol{P_2}\|^2) \quad (4)$$

Using the angular velocity vector of a sphere, we now derive the kinetic energy of **Type-I** (with both rotational axes fixed on the same plane) and **Type-II** (with variable rotational axes) configurations(indicated in **Figure 2** (a)(b)).

### *(A) Case of Type- I*

As shown in **Figure 2** (a), if both rotational axes lie on the same plane, omnidirectional locomotion is possible (see [4]). Therefore, the end point of $\boldsymbol{\omega_1}$ can be determined as the intersection of $l$ (the line perpendicular to the horizontal plane passing through end point $\dot{\boldsymbol{\omega}}$) and $\mathbf{span}\{\boldsymbol{P_1}, \boldsymbol{P_2}\}$. The angle of the sphere's rotational axis $\rho_1$ is then obtained as follows:

$$\rho_1 = \tan^{-1}\left[\frac{(\boldsymbol{P_1} \times \boldsymbol{P_2})_x \sin\varphi - (\boldsymbol{P_1} \times \boldsymbol{P_2})_y \cos\varphi}{(\boldsymbol{P_1} \times \boldsymbol{P_2})_z}\right] \quad (5)$$

By substituting Eqs. (5) into Eqs. (3), we obtain $\boldsymbol{\omega_1}$ as Eqs. (6).

$$\boldsymbol{\omega_1} = \quad (6)$$
$$\frac{\|\boldsymbol{V}\|}{r}\left[-\sin\varphi, \cos\varphi, \frac{(\boldsymbol{P_1} \times \boldsymbol{P_2})_x \sin\varphi - (\boldsymbol{P_1} \times \boldsymbol{P_2})_y \cos\varphi}{(\boldsymbol{P_1} \times \boldsymbol{P_2})_z}\right]^T$$

Substituting Eqs.(6) into Eqs.(4), we obtain $E = E_1$ as Eqs.(7).

$$E_1 = \frac{I}{R^2}(\|\boldsymbol{\omega_1} \times \boldsymbol{P_1}\|^2 + \|\boldsymbol{\omega_1} \times \boldsymbol{P_2}\|^2) \quad (7)$$

### *(B) Case of Type-II*

As shown in **Figure 2** (b), we determine $\rho = \rho_1$, $\boldsymbol{\omega} = \boldsymbol{\omega_2}$ that minimizes the summed kinetic energies of the two rollers, and calculate the minimum energy ($E = E_2$).

To this end, we first express $\boldsymbol{\omega}$ as the sum of $\dot{\boldsymbol{\omega}}$ and $\omega_z \boldsymbol{e_3}$.

$$\boldsymbol{\omega} = \dot{\boldsymbol{\omega}} + \omega_z \boldsymbol{e_3} \quad (8)$$

where

$$\boldsymbol{e_3} = [0, 0, 1]^T, \ \dot{\boldsymbol{\omega}} = [\omega_x, \omega_y, 0]^T \quad (9)$$

And.

$$\boldsymbol{\omega} \times \boldsymbol{P_i} = (\dot{\boldsymbol{\omega}} + \omega_z \boldsymbol{e_3}) \times \boldsymbol{P_i} \quad (10)$$
$$= \dot{\boldsymbol{\omega}} \times \boldsymbol{P_i} + \omega_z(\boldsymbol{e_3} \times \boldsymbol{P_i})$$

$$\|\boldsymbol{\omega} \times \boldsymbol{P_i}\|^2 \quad (11)$$
$$= \langle \dot{\boldsymbol{\omega}} \times \boldsymbol{P_i} + \omega_z(\boldsymbol{e_3} \times \boldsymbol{P_i}), \dot{\boldsymbol{\omega}} \times \boldsymbol{P_i} + \omega_z(\boldsymbol{e_3} \times \boldsymbol{P_i}) \rangle$$
$$= \omega_z^2 \|\boldsymbol{e_3} \times \boldsymbol{P_i}\|^2 + 2\omega_z \langle \dot{\boldsymbol{\omega}} \times \boldsymbol{P_i}, \boldsymbol{e_3} \times \boldsymbol{P_i} \rangle + \|\dot{\boldsymbol{\omega}} \times \boldsymbol{P_i}\|^2$$

Using, Eqs.(11), it is represented as quadratic function with respect to $\omega_z$ as Eqs.(12)

$$\|\boldsymbol{\omega} \times \boldsymbol{P_i}\|^2 + \|\boldsymbol{\omega} \times \boldsymbol{P_i}\|^2 = \quad (12)$$

$$(\|\boldsymbol{e_3}\times\boldsymbol{P_1}\|^2+\|\boldsymbol{e_3}\times\boldsymbol{P_2}\|^2)\omega_z^2 + 2(\langle\dot{\boldsymbol{\omega}}\times\boldsymbol{P_1},\boldsymbol{e_3}\times\boldsymbol{P_1}\rangle+\langle\dot{\boldsymbol{\omega}}\times\boldsymbol{P_2},\boldsymbol{e_3}\times\boldsymbol{P_2}\rangle)\omega_z + \|\dot{\boldsymbol{\omega}}\times\boldsymbol{P_1}\|^2+\|\dot{\boldsymbol{\omega}}\times\boldsymbol{P_2}\|^2$$

Hence, focusing the coefficients of Eqs.(12), $E$ takes minimal value $E_2$ as Eqs.(13).

$$E_2 = (\|\dot{\boldsymbol{\omega}}\times\boldsymbol{P_1}\|^2+\|\dot{\boldsymbol{\omega}}\times\boldsymbol{P_2}\|^2)\frac{I}{R^2} - \frac{(\langle\dot{\boldsymbol{\omega}}\times\boldsymbol{P_1},\boldsymbol{e_3}\times\boldsymbol{P_1}\rangle+\langle\dot{\boldsymbol{\omega}}\times\boldsymbol{P_2},\boldsymbol{e_3}\times\boldsymbol{P_2}\rangle)}{\|\boldsymbol{e_3}\times\boldsymbol{P_1}\|^2+\|\boldsymbol{e_3}\times\boldsymbol{P_2}\|^2} \quad (13)$$

where

$$\omega_z = -\frac{\langle\dot{\boldsymbol{\omega}}\times\boldsymbol{P_1},\boldsymbol{e_3}\times\boldsymbol{P_1}\rangle+\langle\dot{\boldsymbol{\omega}}\times\boldsymbol{P_2},\boldsymbol{e_3}\times\boldsymbol{P_2}\rangle}{\|\boldsymbol{e_3}\times\boldsymbol{P_1}\|^2+\|\boldsymbol{e_3}\times\boldsymbol{P_2}\|^2} \quad (14)$$

$$\rho_2 = \tan^{-1}\left[-\frac{\langle\dot{\boldsymbol{\omega}}\times\boldsymbol{P_1},\boldsymbol{e_3}\times\boldsymbol{P_1}\rangle+\langle\dot{\boldsymbol{\omega}}\times\boldsymbol{P_2},\boldsymbol{e_3}\times\boldsymbol{P_2}\rangle}{\|\boldsymbol{e_3}\times\boldsymbol{P_1}\|^2+\|\boldsymbol{e_3}\times\boldsymbol{P_2}\|^2}\right] \quad (15)$$

Substituting Eqs.(15) into Eqs.(3), $\boldsymbol{\omega_2}$ as Eqs.(16).

$$\boldsymbol{\omega_2} = \frac{\|\boldsymbol{V}\|}{r}\left[-\sin\varphi,\cos\varphi,-\frac{\langle\dot{\boldsymbol{\omega}}\times\boldsymbol{P_1},\boldsymbol{e_3}\times\boldsymbol{P_1}\rangle+\langle\dot{\boldsymbol{\omega}}\times\boldsymbol{P_2},\boldsymbol{e_3}\times\boldsymbol{P_2}\rangle}{\|\boldsymbol{e_3}\times\boldsymbol{P_1}\|^2+\|\boldsymbol{e_3}\times\boldsymbol{P_2}\|^2}\right]^T \quad (16)$$

## 3. Simulation

This section presents the simulation results $\boldsymbol{\omega_1}$(See Eqs.(6)), $\boldsymbol{\omega_2}$ (See Eqs.(16)), $E_1$ (See Eqs.(7)) and $E_2$(See Eqs.(13)) with parameter $\varphi$ ($0° \le \varphi < 360°$) in the given sphere mobile speed: $\|\boldsymbol{V}\| = 1$ [m/s]. The conditions are as follows: $I = 1$, $R = 00.1$[m], $\|\boldsymbol{V}\| = 1$ [m/s], $r = 0.1$[m], $\theta_{1,1} = 215°$, $\theta_{1,2} = 60°, \theta_{2,1} = 325°, \theta_{2,2} = 60°$.

### 3.1 Trajectory of the end point of the angler velocity vector and Totally kinetic energy

This section presents the simulated trajectory of the end points of the angler velocity vectors $\boldsymbol{\omega_1}$and $\boldsymbol{\omega_2}$, and the kinetic energies $E_1$ and $E_2$ .

As shown in Figure 3 (a), the ellipsoid trajectory of $\boldsymbol{\omega_2}$ lies nearer to the $xy$-plane than that of $\boldsymbol{\omega_1}$, and both trajectories cross a common line parallel to the $y$-axis.

As shown in Figure 3 (b), $E_1$ is minimized at sphere direction angles $\varphi =$ 90° and 270°, and maximized at $\varphi = 0°$ and 180°. Meanwhile, $E_2$ is minimized at $\varphi = 0°$ and 180°, and maximized at $\varphi =$ 90° and 270°. And. $E_1$ and $E_2$ are same value at $\varphi =$ 90° and 270°.

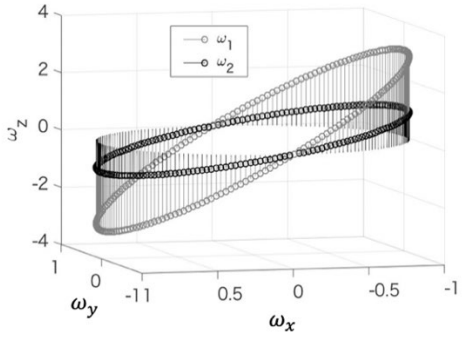


(a)

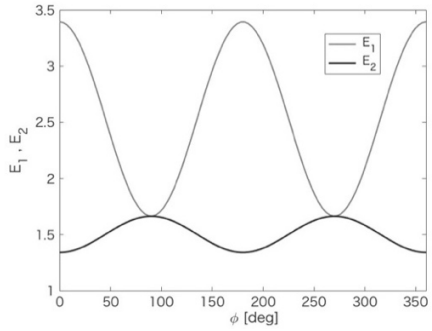


(b)

**Figure 3** Simulation result. (a) Trajectory of angular velocity vector of sphere. (b) Totally kinetic energy

### 3.2 Example of sphere transfer

This subsection simulates the sphere transportation process. As shown in Figure 4, the robot's transfer route starts at $\boldsymbol{O}$ and reaches $\boldsymbol{P}$ and $\boldsymbol{Q}$. Each path $\boldsymbol{OP}$ ($\varphi =$ 90°), $\boldsymbol{PQ}$ ($\varphi = 45°$) and $\boldsymbol{QR}$ ($\varphi = 0°$) is completed after some time $t$ ($0 \le t \le 5$).

The direction angle and mobile speed of the spherical wheel are defined as functions of $t$ (see Figure 5).

$$\varphi(t) = \begin{cases} 90° & 0 \le t \le 5 \\ 45° & 5 \le t \le 10 \\ 0° & 10 \le t \le 15 \end{cases} \quad (17)$$

$$\|\boldsymbol{V}\| = \begin{cases} t & (0 \le t \le 1, 5 \le t \le 6, 10 \le t \le 11) \\ 1 & (1 \le t \le 4, 6 \le t \le 9, 11 \le t \le 14) \\ 5-t & (4 \le t \le 5, 9 \le t \le 10, 14 \le t \le 15) \end{cases} \quad (18)$$

Substituting Eqs. (17) and (18) into Eqs. (6) and (16) respectively, we obtain $\boldsymbol{\omega_1}(t)$ and $\boldsymbol{\omega_2}(t)$, respectively. Moreover, substituting $\boldsymbol{\omega_1}(t)$ and $\boldsymbol{\omega_2}(t)$ into Eqs. (7) and (13) respectively, we obtain $E_1(t)$ and $E_2(t)$, respectively.

The simulation result is shown in **Figure 6**. In the interval $[0, 5]$, the robot is traveling straight, so we have $E_1(t) = E_2(t)$. In the interval $[5, 15]$, $E_2(t)$ is smaller than $E_1(t)$.

**Table 2** The totally kinetic energy efficiency in sphere transport

| Migration pathway | | $OP$ | $PQ$ | $QR$ |
|---|---|---|---|---|
| $[a, b]$ | | $[0, 5]$ | $[5, 10]$ | $[10, 15]$ |
| $\varphi$ | | 90° | 45° | 0° |
| $\boldsymbol{E_i^{[a,b]}}$ | **Type- Ⅰ** | 1.66 | 2.55 | 3.39 |
| | **Type- Ⅱ** | 1.66 | 1.49 | 1.34 |
| $\gamma^{[a,b]}$ | | 0 % | 41 % | 61 % |
| $\gamma^{[0,15]}$ | | 34 % (Total energy reduction ratio) | | |

And. we define integration of $E_1(t), E_2(t)$ with respect to time interval $[a, b]$.

$$\boldsymbol{E_i^{[a,b]}} = \int_a^b E_i(t)\ dx \tag{19}$$

Energy-reduction ratio in $[a, b]$ is defined as follow.

$$\gamma^{[a,b]} = 100(1 - \boldsymbol{E_2^{[a,b]}}/\boldsymbol{E_1^{[a,b]}})\ [\%] \tag{20}$$

As shown in **Table 2**, it is represented by $\gamma^{[0,5]} = 0\ [\%], \gamma^{[5,10]} = 41\ [\%]$ , $\gamma^{[10,15]} = 61\ [\%]$ and is $\gamma^{[0,15]} = 34\ [\%]$. Therefore, the kinetic energy of sphere transport was efficient.

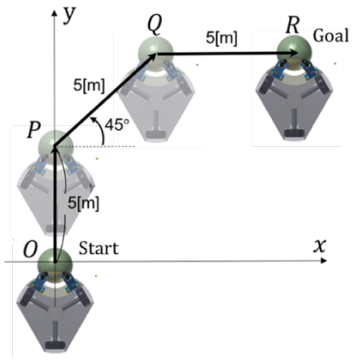


**Figure 4** The robot's transfer route

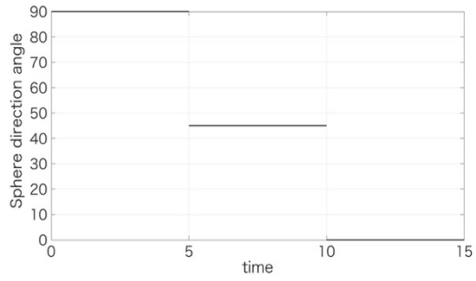


(a)

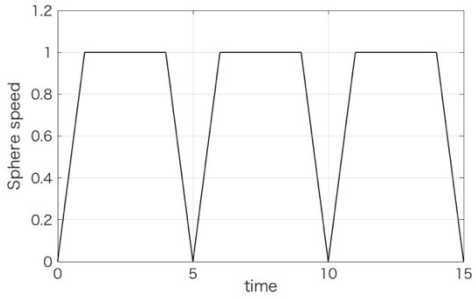


(b)

**Figure 5** The definition (a). Sphere direction (b). Sphere mobile speed

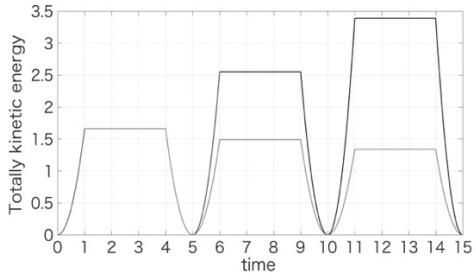


**Figure 6** Simulation result of totally kinetic energy

## 4. Conclusion

We proposed a non-offset mechanism with three-dimensional freedom under the assumption of variable rotational axes of the rollers. The kinetic energy consumption was compared with that of the previous fixed type in a simulation of sphere transportation, which confirmed a large energy reduction in the proposed mechanism.

In future work, we plan to evaluate the kinetic energy of the roller arrangement at an arbitrary contact point on the upper hemisphere as an evaluation function.

## References


[1] M.Wada, K.Kato, "Kinematic modeling and simulation of active-caster robotic drive with a ball transmission (ACROBAT-S)". 2016 IEEE/RSJ International Conference on Intelligent Robots and Systems. Daejeon, 2016-12-9/25, IEEE Robotics and Automation Society,

[2] S.Ishida , H.Miyamoto,"Holonomic Omnidirectional Vehicle with Ball Wheel Drive Mechanism, 2012The JapanSocietyofMechanicalEngineers.Vol.78,No.790, pp.2162-2170, 2012.

[3] S. Chikushi, M. Kuwada, et al., Development of Next-Generation Soccer Robot"Musashi150"for RoboCup MSL,*30th Fussy System Symposium*, pp. 624-627,2014

[4] K. Kimura, K. Ishii, Y. Takemura, M. Yamamoto, Mathematical Modeling and motion analysis of the wheel based ball retaining mechanism, *SCIS & ISIS*, pp.4106-4111, 2016.

[5] K. Kimura, K. Ogata, K. Ishii, Novel Mathematical Modeling and Motion Analysis of a Sphere Considering Slipping, Journal of Robotics, Networking and Artificial Life, Vol.6, issue 1, pp. 27- 32, 2019.

[6] K. Kimura, S. Chikushi, K. Ishii, Evaluation of the Roller Arrangements for the Ball-Dribbling Mechanisms adopted by RoboCup Teams, Journal of Robotics, Nrtworking and Artificial Life, Vol.6, issue 3, pp. 183-190, 2019.

[7] Lee,Y.C,Danny,Lee,D.V.,Chung,J.,andVelinky,S.A.,"Control of a redundant, reconfigurable ball wheel drive mechanism for an omunidirectional platform",Robotica, Cambridge University Press,Vol.25, pp.385-395, 2007.

[8] M. Kumagai, T. Ochiai: "Development of a robot balanced on a ball – Application of passive motion to transport",Proc. ICRA IEEE(2009), pp. 4106-4111, 2009.

[9] Endo, Tatsuro. et al. "An omnidirectional vehicle on a basketball". 12th International Conference on Advanced Robotics. Seattle, 2005-07-18/20, IEEE Robotics and Automation Society, pp. 573-578, 2005.


## Authors Introduction


Dr. Kenji Kimura

He is a Lecturer in National Institute of Technology, Matsue College, where he has been since 2022. He received the ME (mathematics) from Kyusyu University in 2002 and received his Ph.D. degree in engineering from Kyushu Institute of in 2020. Then, He was mathematical teacher of International Baccalaureate Diploma Program (Mathematics) and engineering course chief in Fukuoka Daiichi High School, His research interests spherical mobile robot kinematics, control for object manipulation.

Dr. Kazuo Ishii

He is a Professor in the Kyushu Institute of Technology, where he has been since 1996. He received his Ph.D. degree in engineering from University of Tokyo, Japan, in 1996. His research interests span both ship marine engineering and Intelligent Mechanics. He holds five patents derived from his research. His lab got "Robo Cup 2011 Middle Size League Technical Challenge 1st Place" in 2011. He is a member of the Institute of Electrical and Electronics Engineers, the Japan Society of Mechanical Engineers, Robotics Society of Japan, the Society of Instrument and Control Engineers and so on.